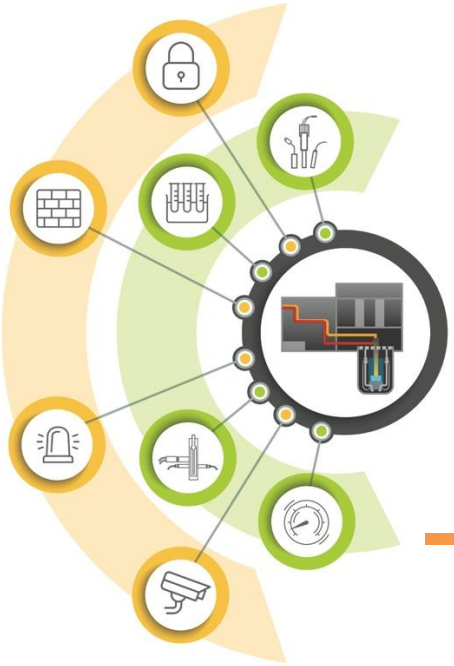

Testing Application of Optical Techniques to Advanced Salt Systems

Prepared for
US Department of Energy

S.D. Branch, H.M. Felmy, S.A. Bryan, and A.M. Lines

Pacific Northwest National Laboratory

September 2023
PNNL-34804

SUMMARY

Molten salt reactors (MSRs) represent a key green energy technology aimed toward meeting increasing work energy demands. Within the United States, support and interest in these reactor designs can be observed, including examples of DOE support through the Advanced Reactor Demonstration Program (ARDP) and GAIN. Significant technological progress is being made with MSR reactor design, but MSRs continue to present a challenging scenario for material and accounting efforts.

A significant effort went into building up the capability for a new glove box. This glove box allows for a more accurate control of the atmospheric conditions, which enables the safe use of higher activity actinides, such as Pu. One of the key observations when working in this glove box is that the molten salts are not subject to higher than acceptable amounts of oxygen and moisture, as evidenced by the persistence of U to remain in the +3 oxidation state and not form the U(VI) species.

Following the standing up of the glove box, the ability to spectroscopically measure U(III) in the presence of a chemically complex environment was demonstrated in a chloride eutectic. This was performed by adding interfering species, including Cr (as a known corrosion product) and Nd (both as a known fission product and surrogate for Pu) into a spectroscopic cell while measuring the spectroscopic signatures of the solution species. The ultraviolet-visible (UV-vis) method followed the ingrowth of the Cr and Nd signatures as the species were added to the chloride eutectic, followed by the ingrowth of the U species. The spectroscopic signatures of each species correlated to what has been reported in the literature. The demonstration of U detection sets the foundation for optical spectroscopic monitoring within an MSR environment. While optical based spectroscopic monitoring cannot achieve the very low uncertainties that traditional offline analysis can, it is important to note the benefits that continuous monitoring can offer for MC&A regarding early detection of complex chemical behavior, such as precipitation.

To further expand the capability of optical monitoring for MC&A, details are included to layout efforts toward integration of a sensor flow cell with an industry partner loop. This includes the installation of intellectual property (IP) protections on both sides and low-hazard aqueous testing with $Nd(NO_3)_3$ in solution to demonstrate the sensor cell's optical performance. The sensor cell was shown to perform well by the UV-vis detection of Nd and the Raman detection of NO_3^-. Considerations for system integration will include slight modifications to the cell design (e.g. welding the cell for seamless connection to the industry partner's flow loop.

This report meets milestone M4RS-23PN0401054, "Testing application of optical techniques to advanced salt systems".

CONTENTS

FIGURES

ACRONYMS AND ABBREVIATIONS

ARDP	Advanced Reactor Demonstration Program
ARS	Advanced reactor safeguards
DOE	US Department of Energy
FY	fiscal year
GAIN	Gateway for Accelerated Innovation in Nuclear
IP	intellectual property
LOD	limit of detection
LWR	light water reactor
MC&A	material control and accounting
MSR	molten salt reactor
PNNL	Pacific Northwest National Laboratory
RMSEP	root mean square error of prediction
UV-vis	ultra-violet visible spectroscopy

1. INTRODUCTION

Molten salt reactors (MSRs) represent a key opportunity to efficiently meet growing green energy needs. As one of the key advanced reactor designs within the United States, designs proposed by various vendors have received media attention and financial support from DOE and through ARDP and GAIN awards. Numerous technological advancements and demonstrations/deployments are currently being completed. Focusing on the liquid fuel reactors, it is important to note that each design represents a major change in how radioactive inventory is spread throughout a facility. This can be further complicated by designs that include on-line refueling, processing, or salt clean up. Overall, traditional material control and accounting (MC&A) approaches used for light water reactors (LWRs) may be difficult to translate to MSR systems.

On-line monitoring may offer a key opportunity to follow these more complex molten salt systems. This not only enables highly representative *in situ* characterization but can provide the unique benefit of continuous monitoring as compared to the discreet and infrequent MC&A completed via grab sample analysis. Furthermore, careful monitoring of system design may also offer a method to catch precipitation or precursors to precipitation that may otherwise impact accurate MC&A. The challenge here is converting monitoring technology that can be applied to the molten salt systems since the temperatures and corrosive environments of MSRs challenge many current system designs.

Fortunately, several technologies can provide highly useful MC&A information and can be adapted to the molten salt environment. A technology of interest here is optical spectroscopy, which can provide unparalleled insight into chemical speciation, redox states, and concentrations in molten salt systems.[1-7] This information can be highly valuable in accurately accounting for actinides that display complex chemistry under molten salt conditions. Furthermore, optical monitoring approaches can be combined with advanced analysis techniques such as chemometric modeling for the real-time and accurate analysis of optical data.[8-14] However, transitioning these technologies to molten salt systems requires key technology advances, which were identified and outlined in previous reports,[14-16] with Figure 1-1 below outlining the key areas. The roadmap in Figure 1-1 summarizes advancements needed to produce a viable tool for MC&A of U,[17] Pu,[18-20] and Np[21] within molten salt systems.

Project work in fiscal year (FY) 2023 was focused on optical spectroscopy as a tool for MC&A of U species within a complex molten salt matrix. Significant efforts went into standing up the capability for a modern glovebox with more accurate control of the oxygen and moisture environment, which are described in Section 2. Upon installation of the new glovebox, the measurement of U within a complex background matrix was demonstrated.[14] Species of interest included Cr, as a corrosion product, and Nd, both as a fission product surrogate and as a model for Pu; this work is discussed in Section 3. This year, efforts included expanding the collaboration with an industry partner, and included the design, fabrication, and testing of a flow cell, capable for future integration within a molten salt micro-loop at TerraPower. This work is summarized in Section 4.

Equipment setup and methodologies are described in Section 2 of this report. Results and discussions of the current work are summarized in Section 3. The conclusions and recommendations are given in Section 4.

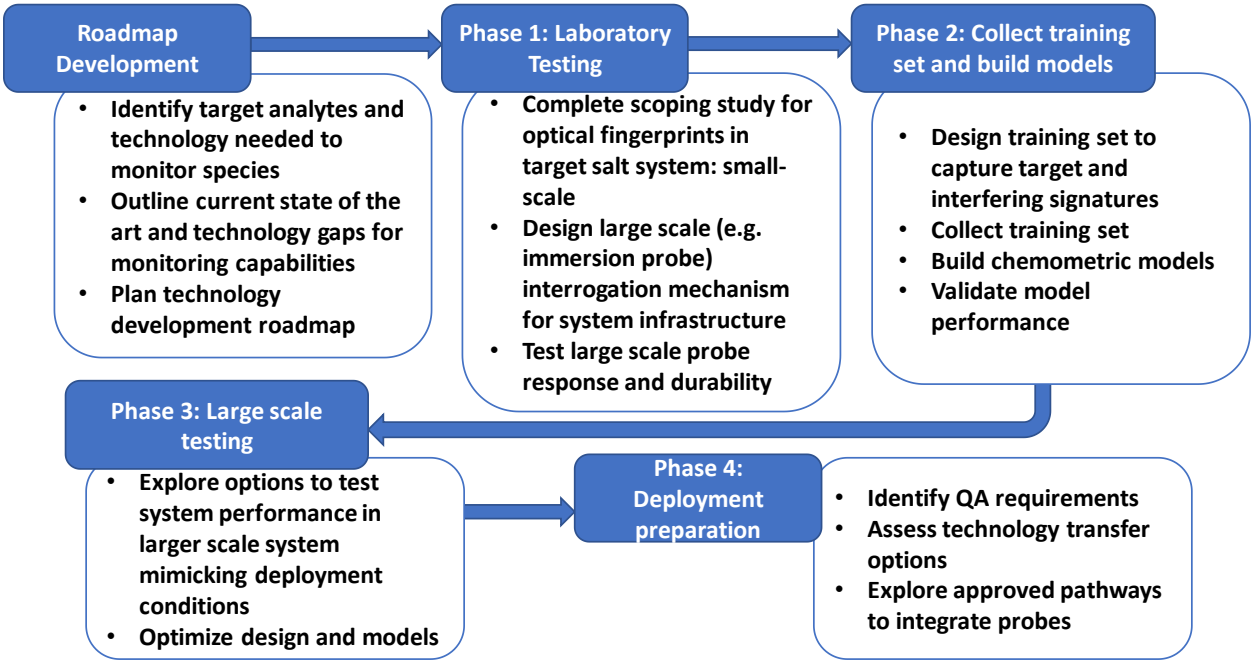

Figure 1-1. Roadmap for on-line monitoring technology development.[16]

2. SETUP AND METHODOLOGIES

Data was shared by collaborators from multiple national laboratories and then used to explore chemometric modeling applicability at PNNL. This section will not provide detail on samples preparation or measurement specifications, as those are more appropriately provided in reports by associated laboratories.

2.1. Reagents and materials

Uranium (III) chloride and a NaCl-$MgCl_2$ salt were acquired from TerraPower. Neodymium (III) chloride was purchased from Thermo, neodymium (III) nitrate was purchased from Strem Chemicals, and chromium (III) chloride was purchased from Sigma Aldrich. All chemicals were used without further purification.

2.2. Modeling

The spectroscopic data were collected into a matrix database within a MATLAB environment (Version: R2022b, MathWorks, Inc., Natick, MA, USA). Multivariate analysis of the spectroscopic data was performed using commercial software (PLS Toolbox, version 9.1, Eigenvector Research Inc., Wenatchee, WA, USA).

2.3. Small-scale molten salt setup

A small-scale furnace system was utilized for this work. The system was based on preexisting setups[3] and modified to allow for better temperature and optical control. Figure 2-1 shows a schematic of the furnace system. The system is designed to hold an optically transparent sample holder (cuvette). In this design, the sample holder has a very long neck to provide a cold finger in order to prevent the molten salt from creeping out of the vessel. Both Raman and UV-vis spectroscopy can be measured simultaneously.

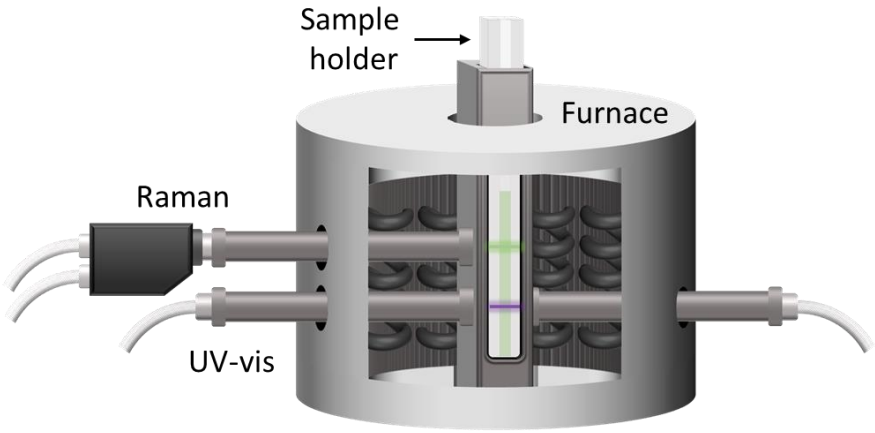

Figure 2-1. Schematic of small-scale furnace system showing vessel inside a clam-shell furnace with both Raman and UV-vis optics connected via fiber optics to the spectroscopic instruments.

Raman and UV-vis spectroscopic instruments were acquired from Spectra Solutions Inc., and each utilized a high throughput volume phase holographic grating spectrograph with a thermoelectrically-cooled two-dimensional charge-coupled device detector. The UV-vis instrument had a functional wavelength range of approximately 450 – 850 nm. The Raman instrument utilized a 532 nm excitation laser with a fiber optic Raman probe with a backscattering (180°) optical design. The wavenumber axis was calibrated using naphthalene and the resolution was <5 cm^{-1}. The wavenumber range is 140 – 4500 cm^{-1}.

2.4. Inert glovebox conditions

All molten salt experiments were conducted in an inert glovebox. The atmosphere in the glovebox is maintained at <0.3 ppm O_2 and <8 ppm moisture. The box pressure is maintained at -1.1" w.c. The inert atmosphere was provided by ultra-high purity argon. Sample holders were thoroughly cleaned and dried at >150 °C prior to being placed into the glovebox.

3. RESULTS AND DISCUSSION

The PNNL team continues to partner with TerraPower to explore and advance applications of optical spectroscopy-based monitoring for MC&A within molten salt reactors. Specific focus is placed on UV-vis and Raman spectroscopy techniques, which are able to provide in-depth information regarding the quantity of target actinides present as well as insight into oxidation state and speciation. While redox and complexation behavior are not traditionally useful information for MC&A, within molten salt reactors this information can indicate if material may be likely to precipitate and impact accuracy of material accounting. The following sections provide an overview of optical fingerprints, expansion of optical libraries to include more complex salt mixtures, and efforts to enable an on-site demonstration of optical probes at a TerraPower facility.

Significant efforts went into standing up the capability for a modern glovebox with more accurate control of the oxygen and moisture environment, which are described in Section 3.1, *Transition to New Inert Containment*.

The measurement of U within a complex background matrix was demonstrated in the presence of added corrosion and fission products. Optical measurements of uranium in molten salt were performed with Cr added as a corrosion product, and Nd added both as a fission product surrogate, and as a model for Pu. This work is described in Section 3.2 *Measurement of U with added corrosion and fission products*.

This FY, efforts included expanding the collaboration with an industry partner, and included the design, fabrication, and testing of a flow cell capable for future integration within a molten salt micro-loop at TerraPower. This work is summarized in Section 3.3. *Design and Development of Flow-Cell for Integration into Molten Salt Flow-Loops.*

3.1. Transition to New Inert Containment

Previous work in molten salts under the ARS campaign was completed within an inert glove box with low limits for actinide concentrations and relatively outdated atmospheric control mechanisms. This FY, while working to determine if PNNL could complete an on-site demo with TerraPower, the PNNL team also took advantage of an opportunity to transition the salt characterization setup into a new glove box. This box exhibits modern atmospheric control mechanisms. It is also approved for working with significantly higher concentrations of actinides, including plutonium. Figure 3-1 below presents pictures of the box along with the PNNL optical characterization system setup within the box.

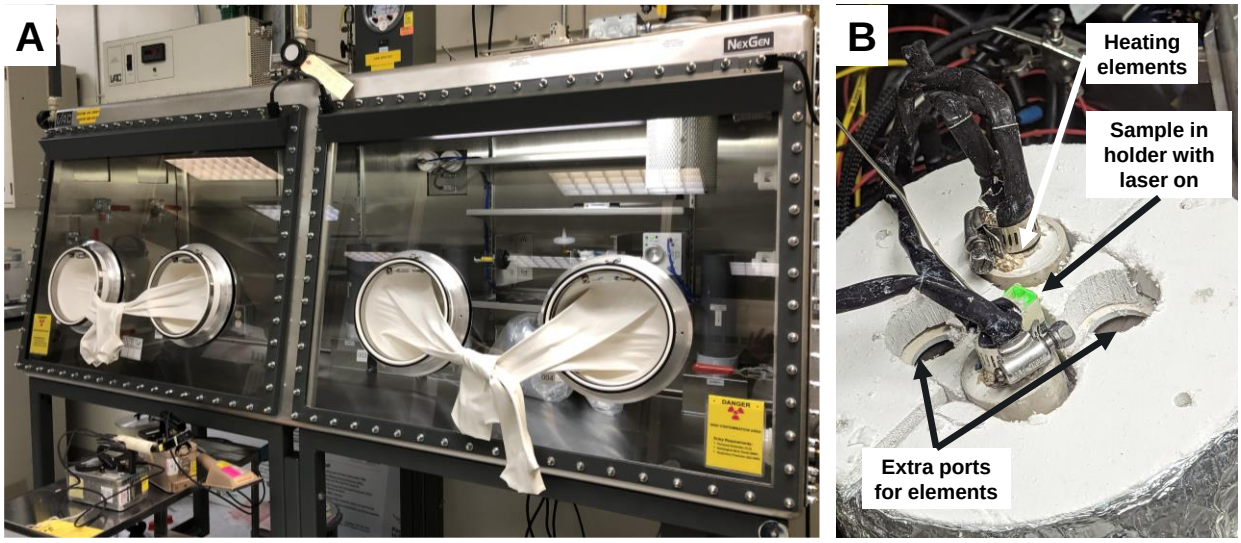

Figure 3-1. A) Photo of new inert glovebox at PNNL. B) Photo of furnace inside inert glovebox.

Transitioning to this new setup represented a significant effort by the PNNL team but was a key opportunity to improve the conditions under which optical techniques for MC&A are tested and developed. Improved atmospheric control will allow the PNNL team to build better data sets that more accurately represent target industry conditions. Furthermore, this new containment can allow for future work to begin focusing on key MC&A targets such as Pu.

3.2. Measurement of U with added corrosion and fission products

This section will provide a brief overview of the unique optical fingerprints of U and interfering species within molten salt systems. Uranium exhibits unique fingerprints in the 3+, 4+, and 6+ oxidation states, where fingerprints will also vary based on speciation and molten salt matrix. For the purposes of work here, and the ultimate target of collaborating with TerraPower to interrogate industry-relevant salts, focus will be placed on chloride salts. More specifically, provided spectra will predominantly feature salt matrices utilizing a NaCl-$MgCl_2$ eutectic provided by TerraPower as the background salt. Figure 3-2 displays the UV-vis spectra of U in the (III), (IV), and (VI) oxidation states and Raman fingerprints of U(VI) as previously observed by the PNNL team.[14, 16] U in the (III) and (IV) oxidations are not Raman active, and therefore have no Raman fingerprints. These optical signatures agree well with literature, particularly when taking into account differences between reported salt matrices and those used here.[22, 23]

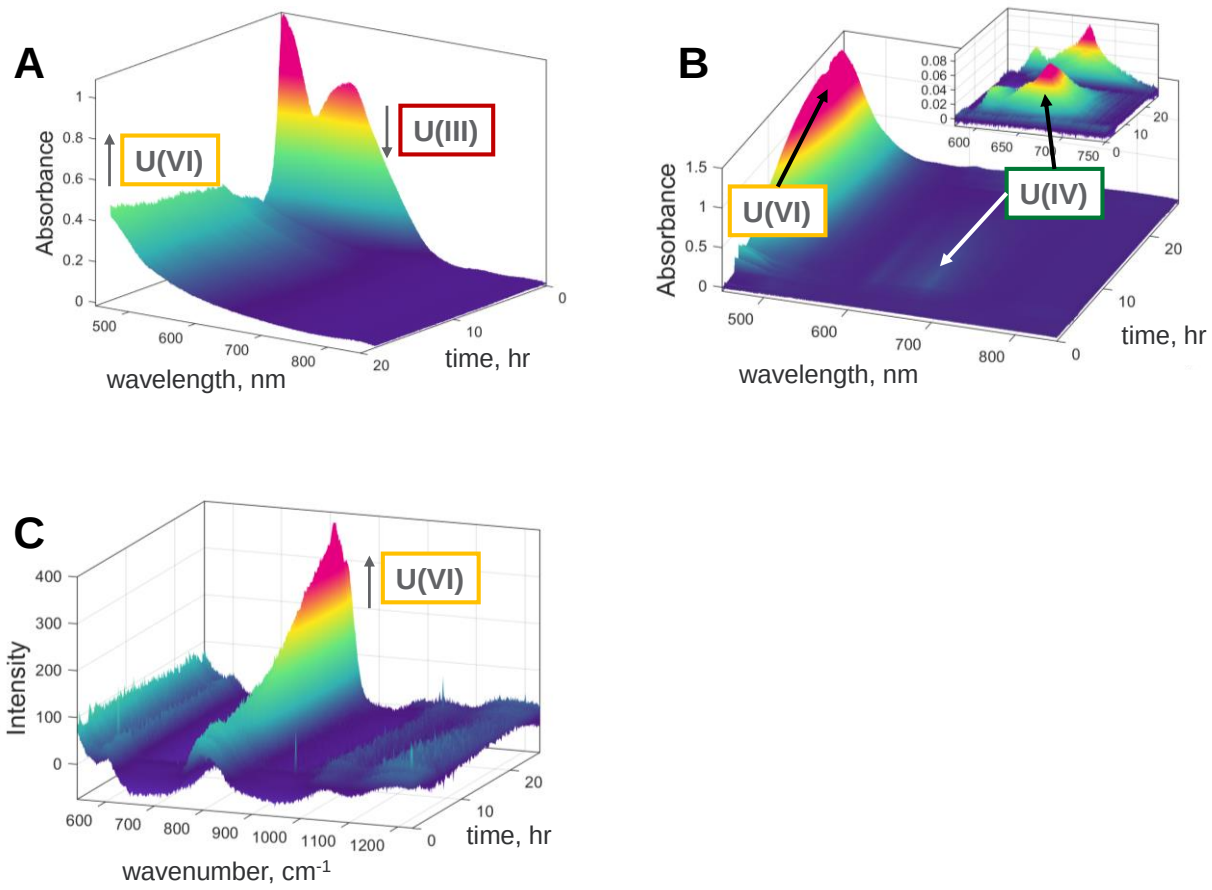

Figure 3-2. A) UV-vis spectra of U(III) and U(VI) in NaCl-$MgCl_2$ collected at 700 °C. B) UV-vis spectra of U(IV) and U(VI) in NaCl-KCl-$MgCl_2$ at 550 °C. C) Raman spectra of U(VI) in NaCl-KCl-$MgCl_2$ at 550 °C. Raman spectra for U(III) and U(IV) have no Raman fingerprint.[16]

It is valuable to note that U will not be the only optically active species in the salt melt. Various fuel species, fission products, and corrosion products will exhibit unique optical fingerprints as well. While this does mean that optical techniques could potentially be utilized to monitor and quantify these targets as well, it also means that signal interferences will be present and data analysis will be complicated. Figure 3-3 presents some literature examples of optical fingerprints within a molten salt in which Nd(III) represents a fission product, Pu(III) represents a fuel species, and Cr(III) represents a corrosion product. Each of these species exhibits a fingerprint that can overlap with U in various oxidation states. The fingerprint for Nd(III) overlaps with U(III), where the molar absorptivity of Nd(III) is ~6 $M^{-1}cm^{-1}$ at ~570 nm,[1] which is over 2 orders of magnitude lower than that of U(III) which is 936 $M^{-1}cm^{-1}$.[23] Nd(III) also has a molar absorptivity of ~3 $M^{-1}cm^{-1}$ at 605 nm which overlaps with U(IV) which has a molar absorptivity of ~5 $M^{-1}cm^{-1}$ at the same wavelength. Pu(III) exhibits multiple fingerprints that overlap U at various oxidation states. The Pu(III) peak at ~480 nm, with a molar absorptivity of ~3 $M^{-1}cm^{-1}$ as well as the peak at ~570 nm with a molar absorptivity of ~7 $M^{-1}cm^{-1}$ overlap with the fingerprints for U(III).[24] The peaks at ~450 nm (~3 $M^{-1}cm^{-1}$), 605 nm (~7 $M^{-1}cm^{-1}$), and 670 nm (~2 $M^{-1}cm^{-1}$) overlap with the fingerprints for U(IV). The peak at ~455 nm (~3 $M^{-1}cm^{-1}$) overlaps with the fingerprint for U(VI). Cr(III) exhibits a broad peak with a maximum at 549 nm with a molar absorptivity of 39.9 $M^{-1}cm^{-1}$.[25] This peak extends from about 475 – 675 nm overlapping with fingerprints of U(III), U(IV), and U(VI).

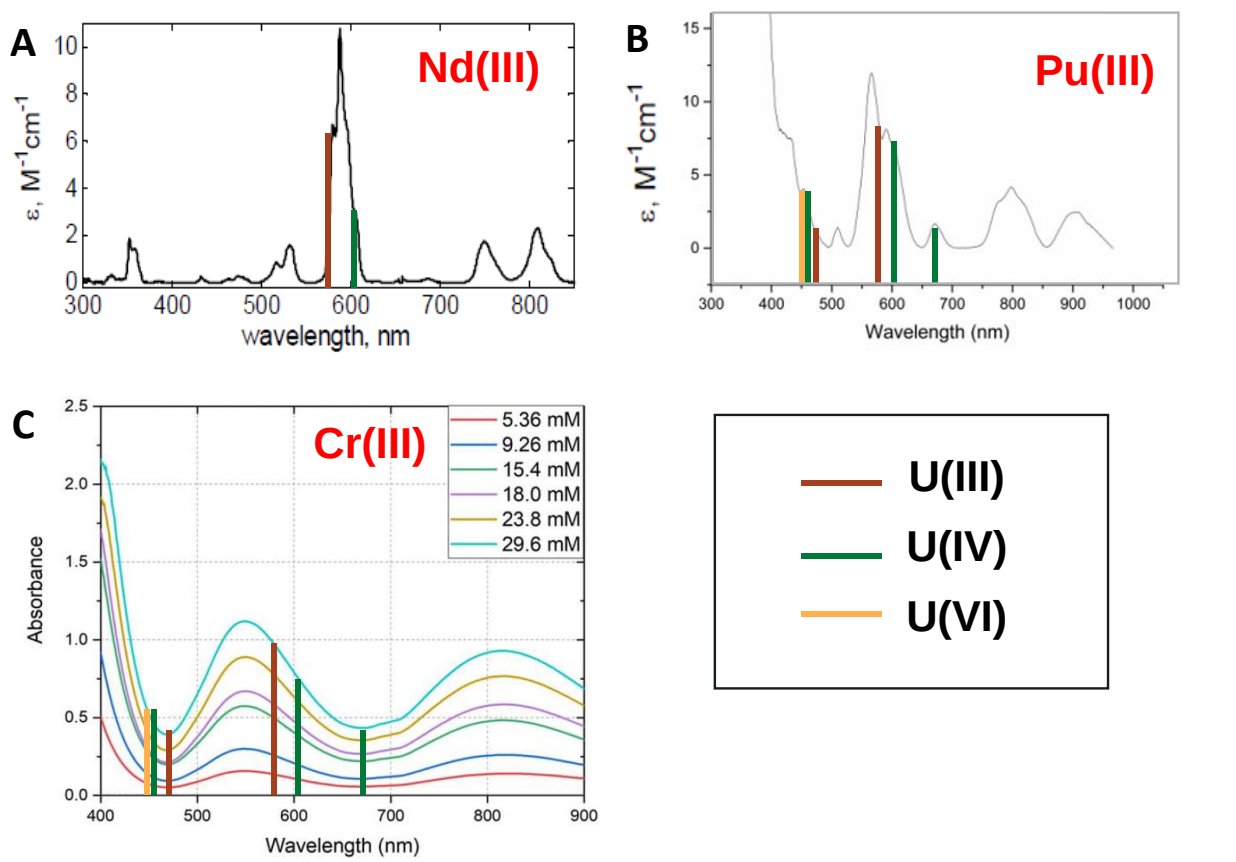

Figure 3-3. Optical fingerprints for select fuel, fission products, and corrosion products found in a molten salt reactor matrix. A) Nd(III) in a molten LiCl-KCl; B) Pu(III) in a molten LiCl-KCl; C) Cr(III) in a molten LiCl-KCl. Legend: The red line represents an optical fingerprint overlap from U(III); green line represents overlap from U(IV), and the yellow line represents overlap from U(VI).

The optical fingerprints of these species can impact the ability of accurate MC&A of the U species if the concentration of each of these species is significantly higher than that of U. One of the strengths of chemometric analysis for online monitoring is the ability to deconvolute complex chemical data using multiple wavelengths for each species. Pu(III), for example, has optical fingerprints into the near-infrared range where the molar absorptivity of U(III) drops significantly.

To explore this further experimentally, the interactions between the fingerprints of U, Nd and Cr were characterized via UV-vis spectroscopy. Figure 3-4 presents the resulting UV-vis spectra. Raman was also recorded, but because the U species of interest is not Raman active, the data is not shown. In this system, $CrCl_3$ was added to a blank NaCl-$MgCl_2$ salt followed by $NdCl_3$ and then UCl_3.

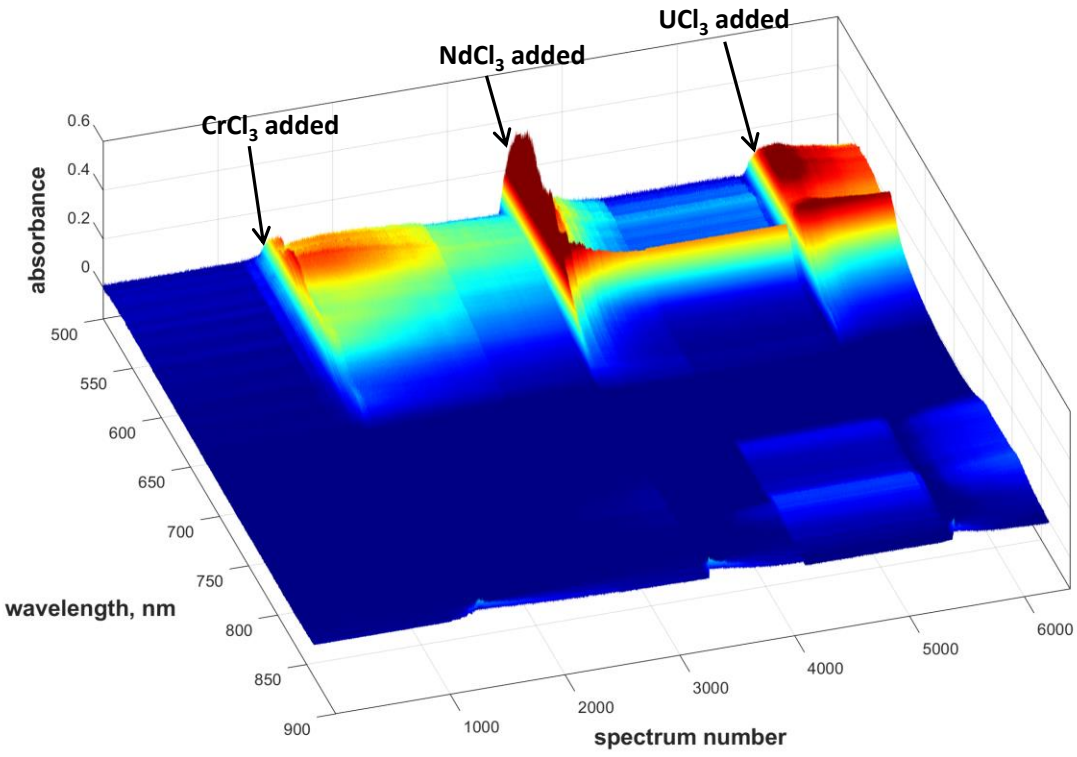

Figure 3-4. UV-vis spectra taken during the addition of $CrCl_3$, $NdCl_3$, and UCl_3 in turn, to a NaCl-$MgCl_2$ molten salt system. Each salt added is indicated within the figure.

The demonstration of characterizing a complex melt presents several key advancements of optical interrogation of molten salts. The ability to track the turbidity of the molten salt due to undissolved solids is potentially an incredibly useful tool for MC&A as it can indicate precipitation within the salt. Formation of solids that can collect in certain parts of the reactor or loop can impact MC&A completed by grab sample analysis. There is not currently a feasible alternative tool available for capturing this. In this experiment, a blank NaCl-$MgCl_2$ salt was heated to 550 °C in an optically transparent cuvette. Each analyte of interest is added by dropping a puck of the reagent into the melt. Each sudden spike in the spectra correlates to the addition of a puck to the sample melt. After each puck addition, the melt becomes turbid, causing the spectrometer to saturate temporarily, until the analyte of interest fully melts within the salt. Cr(III) was added to a total amount of 1.65 wt% of $CrCl_3$, resulting in a transparent, purple melt. The UV-vis spectra shows fingerprints for Cr(III) at ~560 nm and a broad shoulder at ~800 nm, which is consistent with the characteristic fingerprints if Cr(III) in the literature.[25] The presence of Cr demonstrates some of the impacts of potential corrosion products on spectral signal. Following Cr(III), Nd(III) was added to 1.13 wt% in the form of $NdCl_3$, resulting in a bluish-purple melt. Nd(III) shows a fingerprint with 2 peaks at ~580 nm and ~590 nm, and fingerprints with small, sharp peaks at ~750 nm and ~810 nm. This is consistent with the literature values for Nd(III) in a similar salt matrix.[1] Measurement of Nd serves as a good model for monitoring Pu, which provides a valuable foundation for testing in the next FY.

Following Nd(III), U(III) was added to 0.53 wt% in the form of UCl_3. Upon addition of U(III), the melt became turbid while the U(III) dissolved. After an hour, the optical fingerprints of U(III) were observed, with a broad peak observed at ~570 nm, which is consistent with the literature for U(III) in a similar

matrix.[23] Figure 3-5 calls out select spectra from Figure 3-4 highlighting the unique optical fingerprints for each species.

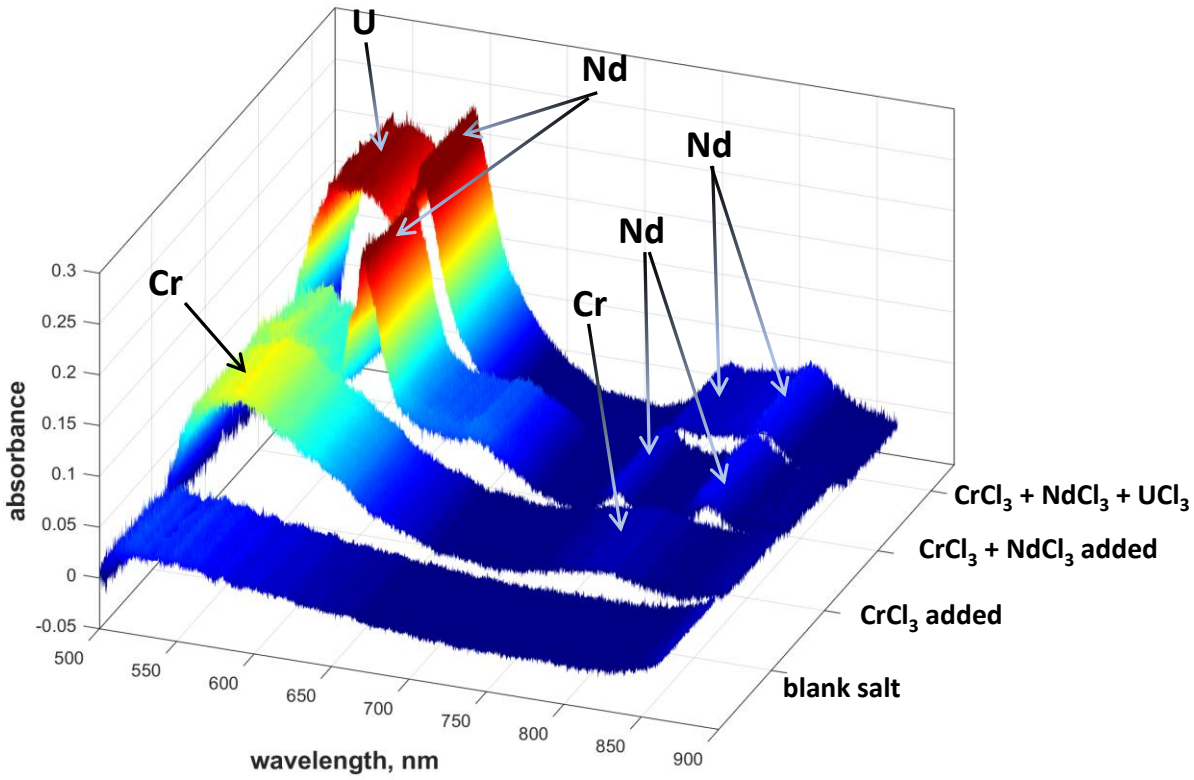

Figure 3-5. Selected UV-vis spectra containing blank NaCl-$MgCl_2$ eutectic salt, and salt containing $CrCl_3$, $CrCl_3$ + $NdCl_3$, and $CrCl_3$ + $NdCl_3$ + UCl_3 in solution. The individual bands associated with each metal constituent are labeled within the figure.

The addition of Cr, combined with the addition of Nd, creates a highly complex signal background to which U is added. The ability to even qualitatively parcel out U signal on top of this complex optical background is a major step forward for showing how optical tools can be leveraged in industry-relevant salts. What is important to observe in this data is the persistent presence of U(III) and absence of the U(VI) signature in the salt matrix. This is indicative of more up-to-date atmospheric control within the new glovebox.

3.3. Design and Development of Flow-Cell for Integration into Molten Salt Flow-Loops

To effectively demonstrate the utility of MC&A on-line monitoring tools, the goal is to integrate optical sensors into industrial molten salt processes. A particularly valuable opportunity includes integration of PNNL sensors into a TerraPower micro-loop. This provides a venue to test probe performance under realistic operating conditions looking at real industry salts. Towards that end, PNNL has been collaborating with TerraPower to identify probe integration opportunities. Ultimately, completing a demo in FY23 did

not align with industry targets. We are recommending testing under industry representative conditions with a commercial partner.

In support of these efforts, PNNL completed an FY23 task to design a sensor flow cell that could be incorporated into a TerraPower or another commercial partner micro-loop. Figure 3-6 below provides a photo of the cell. Note, details in this photo are presented at a very high level. The PNNL team worked with a small business partner to design the cell. The small business vendor plans to include this cell in their commercial products following demonstration and testing on salts.

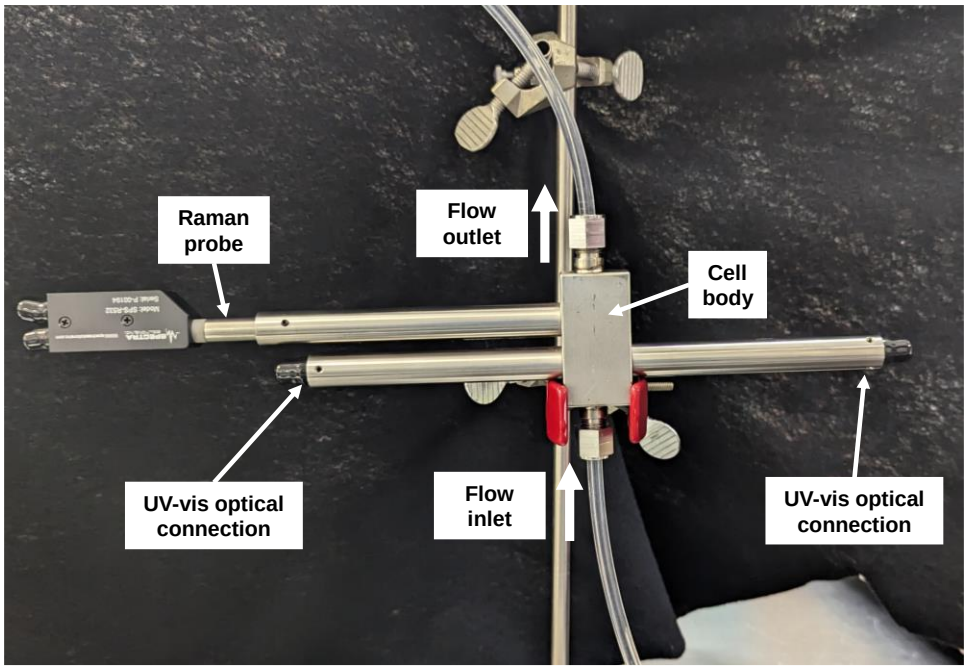

Figure 3-6. Photo of the optical flow cell.

In preparation for testing on TerraPower salt loops, the sensor cell response was tested under aqueous conditions. This allowed for a lower-hazard test loop to be setup where targets/simulants such as Nd could readily be added. Various concentrations of $Nd(NO_3)_3$ in water were flowed through the cell body using a syringe pump. Each sample was flowed through for ~5 minutes before optical collection to ensure accurate sample concentration at time of measurement. After optical collection, the sample was pulled from the flow cell and replaced with the next sample. Figure 3-7 presents an example of the Raman and UV-vis response to a series of $Nd(NO_3)_3$ solutions being introduced into the sensor cell. Nd(III) has a unique UV-vis spectral fingerprint but does not have a strong Raman response. NO_3^- does have a strong Raman signature, however. Figure 3-7 therefore demonstrates the UV-vis signal of Nd(III) and the Raman signal of NO_3^-.

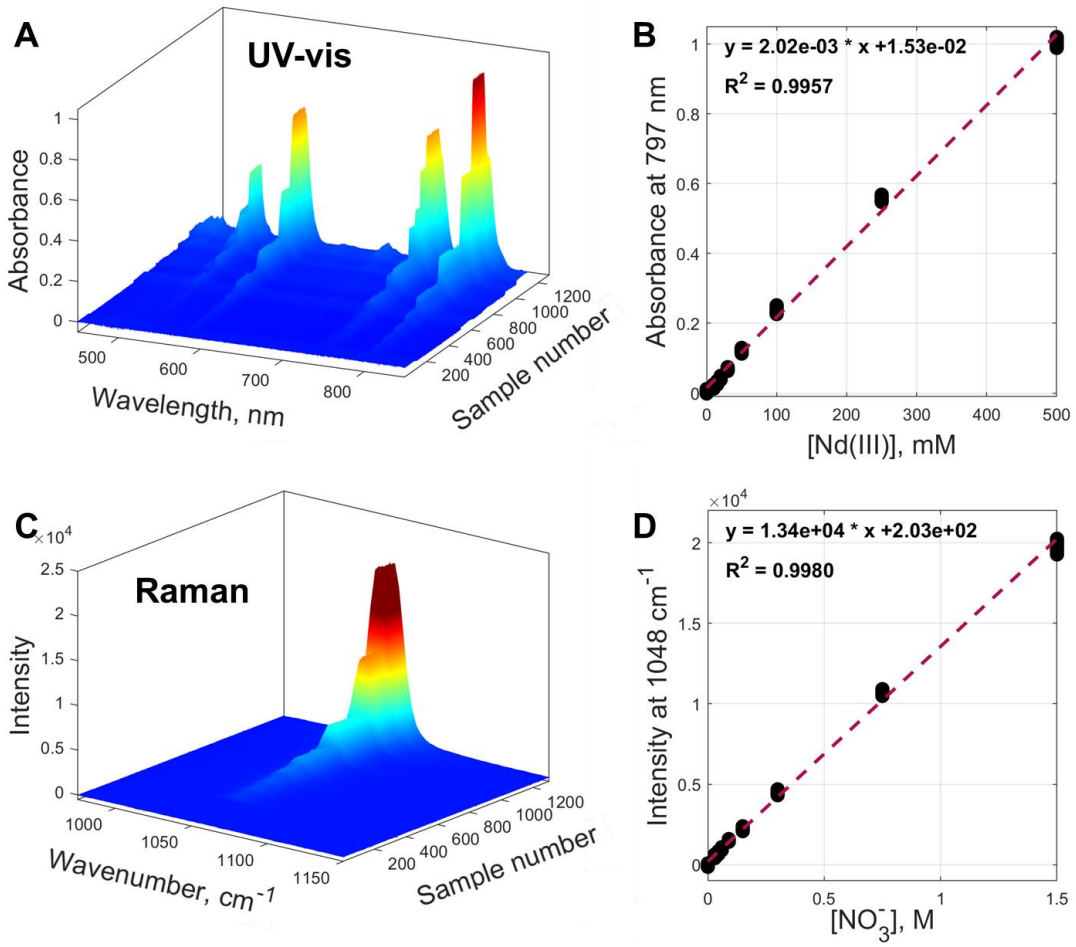

Figure 3-7. Test of the flow cell with 0 – 500 mM $Nd(NO_3)_3$ at 0 mL/min (static conditions) showing A) a 3D plot of UV-vis spectra with increasing concentration, B) calibration curve of Nd(III) absorbance at 797 nm as a function of concentration, C) 3D plot of Raman spectra highlighting the NO_3^- band, and D) the resulting calibration curve of the intensity of the NO_3^- band at 1048 cm^{-1} as a function of NO_3^- concentration.

Under aqueous conditions, the cell is seen to perform well. No leaks were observed and optical output from both UV-vis and Raman was good. As shown in Figure 3-7 above, sensor response was linear with concentration, producing well behaved single variate calibration curves. The spectral response for Nd(III) at 797 nm and NO_3^- at 1048 cm^{-1} are consistent with signatures reported in the literature.[26] Optical spectra were recorded for the Nd(III) solutions flowing through the sensor cell at 0, 0.5, and 1 mL/min, and are shown in Figure 3-8A and Figure 3-8B. As expected, the spectral response showed no observable difference between 0.5 mL/min or 1.0 mL/min flow-rate.

The chemometric model for the prediction of Nd(III) based on the static UV-vis measurements was prepared, and the parity plot showing the performance is shown in Figure 3-8C. This model was used to predict the concentrations of the $Nd(NO_3)_3$ concentration for the flow tests at 0.5 mL/min and 1.0 mL/min flow rates (Figure 3-8A and Figure 3-8B, respectively). The results of the predictions are sown in Figure 3-9A and Figure 3-9B for the two respective flow rates. The root-mean-square-error for prediction (RMSEP) for the 0.5 mL/min and 1.0 mL/min flow tests are 6.296 mM and 7.588 mM respectively, which corresponds to ~1.5 % relative error of measurement.

In preparation for planned FY24 on-site demos, the cell design may be modified slightly to allow the cell to be welded in place as opposed to connected into the loop via swage fittings.

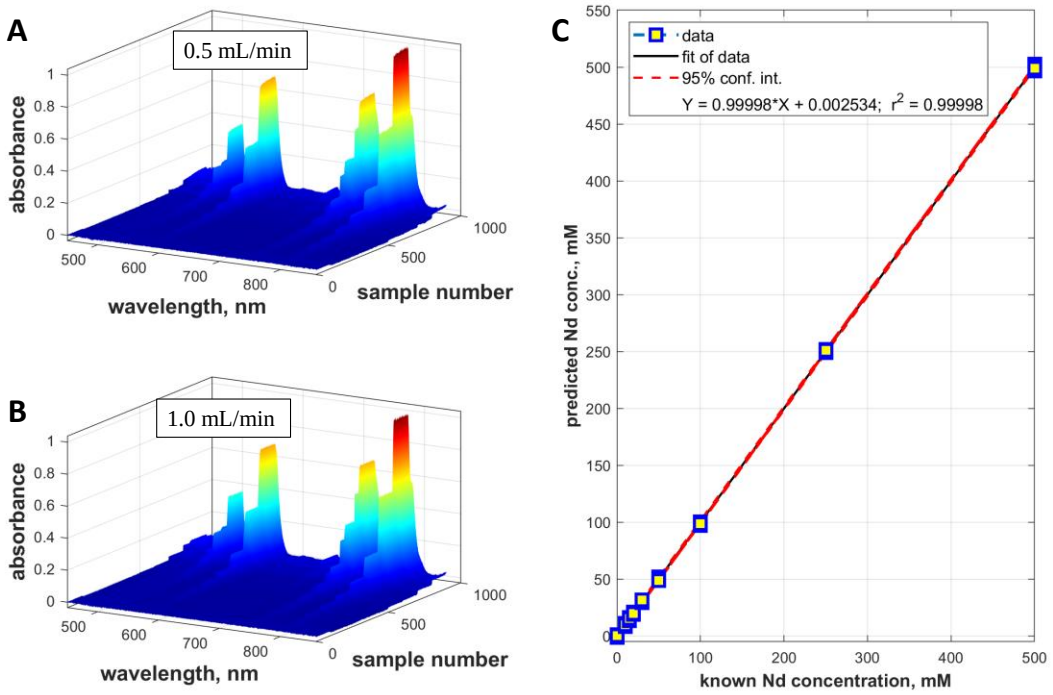

Figure 3-8. Test of the flow cell with 0 – 500 mM $Nd(NO_3)_3$ at 0.5 mL/min (flow conditions), and B) at 1.0 mL/min (flow conditions). C) Parity plot showing the predicted vs the known concentration of $Nd(NO_3)_3$, in the flow cell measured by UV-vis under flowing conditions.

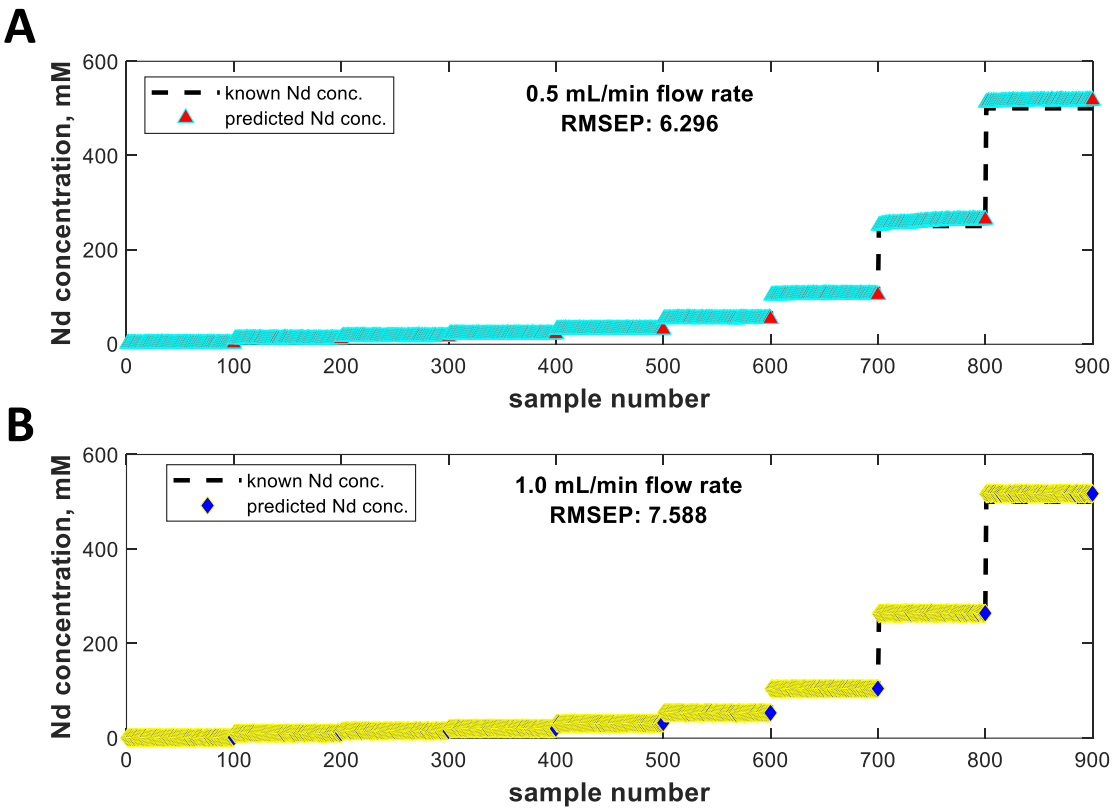

Figure 3-9. Flow test showing the on-line measurement of the validation test dataset under flowing conditions at A) 0.5 mL/min and B) 1.0 mL/min.

4. CONCLUSIONS AND RECOMMENDATIONS

Optical spectroscopy based on-line monitoring can be a powerful tool to support comprehensive MC&A of MSRs and supporting systems. In particular, sensors utilizing UV-vis and Raman spectroscopy can be adapted to molten salt applications to provide unparalleled insight into salt composition, including providing information on oxidation state and speciation. While isotopics are typically a primary focus of MC&A, optical monitoring of the complex chemistry within molten salt systems can allow for better understanding of physical phenomena of precipitation or plating out of materials that could impact accuracy of MC&A results. Here, the expansion of optical applications to molten salts is discussed with the characterization of U in the presence of interfering species such as Nd and Cr.

PNNL advanced opportunities and capabilities in two major areas during FY23. First the PNNL team transitioned their existing characterization system into a new inert glove box. This modern system allows for better atmospheric control and can support the future analysis of higher concentrations of U as well as characterization of other actinides, including Pu. Secondly, PNNL is collaborating with industry to organize on-site testing of optical sensors within industry representative salt systems. Planning for installing an optical sensor cell into an industrial loop is underway. In support of these efforts, PNNL designed, procured,

and tested a sensor flow cell for use in an industry micro-loop. This sensor was tested on aqueous systems to check for leaks and characterize optical output. Sensor performance was excellent, and only minor modifications expected to support sensor cell integration in the future (e.g. modifying the cell so it can be welded into a micro-loop). Overall, optical approaches can be valuable for MSR MC&A, where the current state of the art of sensor technology is being advanced to meet system needs.

5. ACKNOWLEDGEMENTS

This work was funded by the Department of Energy Office of Nuclear Energy's Advanced Reactor Safeguards Campaign. Pacific Northwest National Laboratory (PNNL) is operated by Battelle Memorial Institute for the DOE under contract DE-AC05-76RL01830.

The team would also like to acknowledge and thank TerraPower for providing a variety of salt samples allowing the team to explore applications to representative salt systems.

6. REFERENCES

(1) Schroll, C. A.; Lines, A. M.; Heineman, W. R.; Bryan, S. A. Absorption spectroscopy for the quantitative prediction of lanthanide concentrations in the 3LiCl-2CsCl eutectic at 723 K. *Analytical Methods* **2016**, *8* (43), 7731-7738, 10.1039/C6AY01520D. DOI: 10.1039/c6ay01520d.
(2) Schroll, C. A.; Chatterjee, S.; Levitskaia, T. G.; Heineman, W. R.; Bryan, S. A. Electrochemistry of Europium(III) Chloride in 3 LiCl - NaCl, 3 LiCl-2 KCl, LiCl - RbCl, and 3 LiCl-2 CsCl Eutectics at Various Temperatures. *Journal of the Electrochemical Society* **2017**, *164* (8), H5345-H5352. DOI: 10.1149/2.0521708jes.
(3) Schroll, C. A.; Chatterjee, S.; Levitskaia, T. G.; Heineman, W. R.; Bryan, S. A. Electrochemistry and Spectroelectrochemistry of europium(III) chloride in 3LiCl-2KCl from 643 to 1123 K. *Anal Chem* **2013**, *85* (20), 9924-9931. DOI: 10.1021/ac402518p From NLM PubMed-not-MEDLINE.
(4) Schroll, C. A.; Chatterjee, S.; Levitskaia, T.; Heineman, W. R.; Bryan, S. A. Spectroelectrochemistry of EuCl3 in Four Molten Salt Eutectics; 3 LiCl-NaCl, 3 LiCl-2 KCl, LiCl-RbCl, and 3 LiCl-2 CsCl; at 873 K. *Electroanalysis* **2016**, *28* (9), 2158-2165. DOI: 10.1002/elan.201600048.
(5) Polovov, I. B.; Volkovich, V. A.; Charnock, J. M.; Kralj, B.; Lewin, R. G.; Kinoshita, H.; May, I.; Sharrad, C. A. In situ spectroscopy and spectroelectrochemistry of uranium in high-temperature alkali chloride molten salts. *Inorg Chem* **2008**, *47* (17), 7474-7482. DOI: 10.1021/ic701415z.
(6) Park, Y. J.; Bae, S. E.; Cho, Y. H.; Kim, J. Y.; Song, K. UV-vis absorption spectroscopic study for on-line monitoring of uranium concentration in LiCl-KCl eutectic salt. *Microchemical Journal* **2011**, *99* (2), 170-173. DOI: 10.1016/j.microc.2011.04.013.
(7) Nagai, T.; Uehara, A.; Fujii, T.; Yamana, H. Reduction behavior of UO22+ in molten LiCl-RbCl and LiCl-KCl eutectics by using tungsten. *Journal of Nuclear Materials* **2013**, *439* (1-3), 1-6. DOI: 10.1016/j.jnucmat.2013.03.078.
(8) Bryan, S. A.; Levitskaia Tatiana, G.; Johnsen, A. M.; Orton, C. R.; Peterson, J. M. Spectroscopic monitoring of spent nuclear fuel reprocessing streams: an evaluation of spent fuel solutions via Raman, visible, and near-infrared spectroscopy. In *Radiochimica Acta International journal for chemical aspects of nuclear science and technology*, 2011; Vol. 99, p 563.
(9) Lines, A. M.; Hall, G. B.; Asmussen, S.; Allred, J.; Sinkov, S.; Heller, F.; Gallagher, N.; Lumetta, G. J.; Bryan, S. A. Sensor Fusion: Comprehensive Real-Time, On-Line Monitoring for Process Control via Visible, Near-Infrared, and Raman Spectroscopy. *ACS Sens* **2020**, *5* (8), 2467-2475. DOI: 10.1021/acssensors.0c00659.
(10) Lines, A. M.; Hall, G. B.; Sinkov, S.; Levitskaia, T.; Gallagher, N. B.; Lumetta, G. J.; Bryan, S. A. Overcoming Oxidation State-Dependent Spectral Interferences: Online Monitoring of U(VI) Reduction to U(IV) via Raman and UV-vis Spectroscopy. *Ind Eng Chem Res* **2020**, *59* (19), 8894-8901. DOI: 10.1021/acs.iecr.9b06706.
(11) Lines, A. M.; Nelson, G. L.; Casella, A. J.; Bello, J. M.; Clark, S. B.; Bryan, S. A. Multivariate Analysis To Quantify Species in the Presence of Direct Interferents: Micro-Raman Analysis of HNO(3) in Microfluidic Devices. *Anal Chem* **2018**, *90* (4), 2548-2554. DOI: 10.1021/acs.analchem.7b03833 From NLM PubMed-not-MEDLINE.
(12) Lines, A. M.; Tse, P.; Felmy, H. M.; Wilson, J. M.; Shafer, J.; Denslow, K. M.; Still, A. N.; King, C.; Bryan, S. A. Online, Real-Time Analysis of Highly Complex Processing Streams: Quantification of Analytes in Hanford Tank Sample. *Industrial & Engineering Chemistry Research* **2019**, *58* (47), 21194-21200. DOI: 10.1021/acs.iecr.9b03636.
(13) Tse, P.; Bryan, S. A.; Bessen, N. P.; Lines, A. M.; Shafer, J. C. Review of on-line and near real-time spectroscopic monitoring of processes relevant to nuclear material management. *Anal Chim Acta* **2020**, *1107*, 1-13. DOI: 10.1016/j.aca.2020.02.008.
(14) Branch, S. D.; Felmy, H. M.; Schafer Medina, A.; Bryan, S. A.; Lines, A. M. Exploring the Complex Chemistry of Uranium within Molten Chloride Salts. *Ind Eng Chem Res* **2023**. DOI: 10.1021/acs.iecr.3c02005.

(15) Paviet, P.; Hartmann, T.; Lines, A. M.; Bryan, S. A.; Felmy, H. M.; Glezakou, V.-A.; Nguyen, M.-T.; Medina, A.; Branch, S. D. *Corrosion of Molten Salt Containment Alloys - Fundamental Mechanisms for Corrosion Control and Monitoring*; Pacific Northwest National Laboratory, Richland, Washington, 2020.
(16) Lines, A. M.; Bryan, S. A.; Felmy, H. M.; Branch, S. D. On-line Monitoring for Molten Salt Reactor MC&A: Optical Spectroscopy-Based Approaches, PNNL-33367. Pacific Northwest National Laboratory: Richland, WA, 2022.
(17) Nagai, T.; Uehara, A.; Fujii, T.; Yamana, H. Reduction behavior of UO_2^{2+} in molten LiCl – RbCl and LiCl – KCl eutectics by using tungsten. *Journal of Nuclear Materials* **2013**, *439* (1), 1-6. DOI: https://doi.org/10.1016/j.jnucmat.2013.03.078.
(18) Shirai, O.; Iwai, T.; Suzuki, Y.; Sakamura, Y.; Tanaka, H. Electrochemical behavior of actinide ions in LiCl–KCl eutectic melts. *Journal of Alloys and Compounds* **1998**, *271-273*, 685-688. DOI: https://doi.org/10.1016/S0925-8388(98)00187-X.
(19) Serp, J.; Konings, R. J. M.; Malmbeck, R.; Rebizant, J.; Scheppler, C.; Glatz, J. P. Electrochemical behaviour of plutonium ion in LiCl–KCl eutectic melts. *J Electroanal Chem* **2004**, *561*, 143-148. DOI: https://doi.org/10.1016/j.jelechem.2003.07.027.
(20) Bourgès, G.; Lambertin, D.; Rochefort, S.; Delpech, S.; Picard, G. Electrochemical studies on plutonium in molten salts. *Journal of Alloys and Compounds* **2007**, *444-445*, 404-409. DOI: 10.1016/j.jallcom.2006.10.095.
(21) Polovov, I. B.; Sharrad, C. A.; May, I.; Vasin, B. D.; Volkovich, V. A.; Griffiths, T. R. Spectroelectrochemical Study of Uranium and Neptunium in LiCl-KCl Eutectic Melt. *ECS Transactions* **2007**, *3* (35), 503-511.
(22) Nagai, T.; Fujii, T.; Shirai, O.; Yamana, H. Study on Redox Equilibrium of UO22+/U2+in Molten NaCl-2CsCl by UV-Vis Spectrophotometry. *Journal of Nuclear Science and Technology* **2004**, *41* (6), 690-695. DOI: 10.1080/18811248.2004.9715534.
(23) Nagai, T.; Uehara, A.; Fujii, T.; Shirai, O.; Sato, N.; Yamana, H. Redox equilibrium of U4+/U3+ in molten NaCl-2CsCl by UV-Vis spectrophotometry and cyclic voltammetry. *Journal of Nuclear Science and Technology* **2005**, *42* (12), 1025-1031. DOI: DOI 10.3327/jnst.42.1025.
(24) Lambert, H. Molten salt spectroscopy and electrochemistry for spent nuclear fuel treatment. The University of Manchester (United Kingdom), 2017.
(25) Yoon, S.; Choi, S. Spectroelectrochemical Behavior of Cr, Fe, Co, and Ni in LiCl-KCl Molten Salt for Decontaminating Radioactive Metallic Wastes. *Journal of The Electrochemical Society* **2021**, *168* (1), 013504. DOI: 10.1149/1945-7111/abdc7e.
(26) Nelson, G. L.; Lines, A. M.; Bello, J. M.; Bryan, S. A. Online Monitoring of Solutions Within Microfluidic Chips: Simultaneous Raman and UV–Vis Absorption Spectroscopies. *ACS Sensors* **2019**, *4* (9), 2288-2295. DOI: 10.1021/acssensors.9b00736.